Suppression of Leakage Current and Distortion in Variable Capacitance Devices and their Application to AC Power Regulators

Akihiko Katsuki[†] and Takuya Oki[*]

[†]Next Generation Switching Power Course, Nagasaki University, Nagasaki, Japan
[*]Department of Computer Science and Electronics, Kyushu Institute of Technology, Iizuka-shi, Fukuoka, Japan

Abstract

The quantity of alternating current (AC) leakage and the value of distortion factor in capacitor currents are discussed with regard to a new power component called variable capacitance device (VCD). This component has terminals for controlling its capacitance. Nonlinear dielectric characteristics are utilized in this device to vary the capacitance. When VCD operates in an AC circuit, the AC leakage from this device through direct current (DC) control voltage source increases according to the conditions of DC control voltage and so on. To solve this problem, we propose techniques for suppressing AC leakage. Although VCD has strong nonlinear characteristics, the current through the capacitor is not distorted significantly. The relations between AC leakage and the distortion in current waveforms are investigated. An application example for an AC power regulator is also introduced to evaluate the distortion in waveforms.

Key words: AC power regulator, Current distortion, DC control voltage, Leakage current, Variable capacitance device

I. INTRODUCTION

If power devices of variable capacitance can be used, then many applications will be possible in the field of power electronics. In alternating current (AC) voltage regulators, such as ferroresonant circuit, inductances are usually varied to control output voltage. A simulated saturating reactor [1] is assembled by a small inductor and semiconductor switches. A voltage regulator with this circuit has a reduced size and weight in comparison with a ferroresonant transformer [2]. However, considerable magnetic fields are generated, thereby causing electronic equipment to malfunction. This condition is not desirable for a clean and safe environment.

Varactors are passive components that can vary their capacitance. However, they have a small operating current (e.g., less than approximately 10 μA) because they are basically reverse-biased diodes. Therefore, their application is limited to small signal use.

Variable capacitance device (VCD) [3], [4] is proposed on the supposition that the value of an operating current is several amperes or more. This device is realized by using the capacitance varying characteristics of direct current (DC) bias voltage across a ceramic capacitor [5]–[7].

A ceramic capacitor has nonlinearity in the characteristics between dielectric constant and electric field, that is, those between capacitance and DC bias voltage. Ceramic capacitors are usually used in the circuit with a fixed DC bias voltage to avoid this influence. However, the influence of nonlinearity on the use of such capacitors in AC circuits cannot be neglected.

In this study, the major problems on the use of ceramic capacitors in AC circuits, that is, AC leakage from VCD to DC controlling voltage source, and waveform distortion are investigated in detail. Leakage current suppression techniques can be applied to AC power regulators. With respect to an AC power regulator with constant voltage/constant current (CV/CC), the relationship between AC leakage suppression technique and waveform distortion is reported, including the observed waveforms and measured data on efficiency.
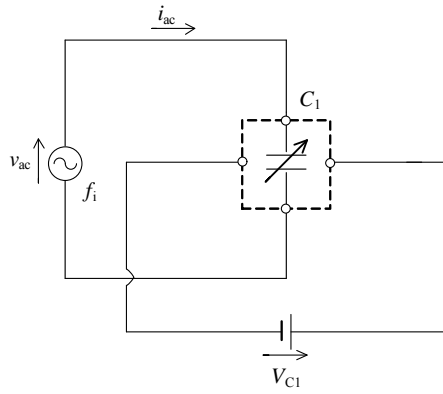
Fig. 1. VCD.
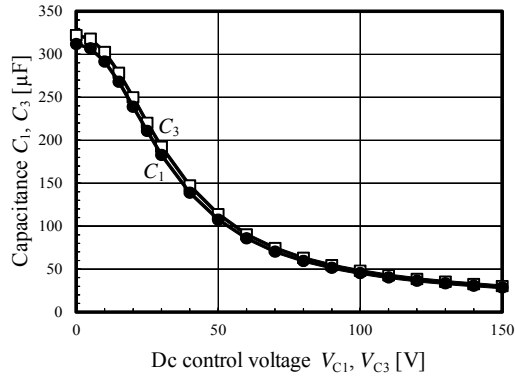
Fig. 2. Example of measured control characteristics in VCDs.

Fig. 3. Structure of a VCD.

Fig. 4. Leakage current suppression in the VCD.

II. VCD

We introduce the use of VCD in an AC circuit. The circuit symbol of VCD is depicted in Fig. 1. Fig. 2 presents an example of the measured data between capacitance C_1 and DC control voltage V_{C1}, in which the AC current for measurement is sufficiently small. Fig. 2 shows that the capacitances can be adjusted by changing DC control voltage.

The structure of a four-terminal VCD is depicted in Fig. 3. Four capacitors C_A, C_B, C_C, and C_D have the same characteristics. With the use of two resistors R_B, the same DC voltages are imposed on the four capacitors.

III. LEAKAGE CURRENT SUPPRESSION

In Fig. 3, the voltages v_A, v_B, v_C, and v_D across the capacitors C_A, C_B, C_C, and C_D can be expressed by V_{C1} and the AC voltage v_{ac} as follows:

$$v_A = v_D = \frac{V_{C1} + v_{ac}}{2} \tag{1}$$

$$v_B = v_C = \frac{V_{C1} - v_{ac}}{2} \tag{2}$$

The DC control voltage source V_{C1} has low impedance against AC. In this study, its impedance is assumed to be zero.

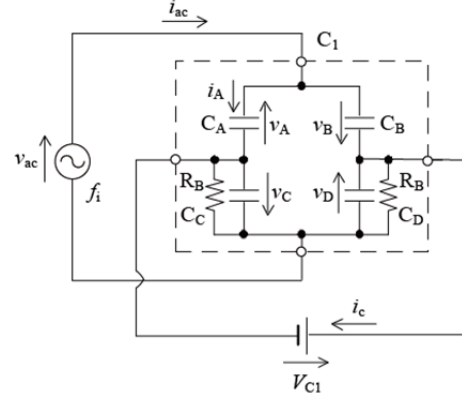The bridge connection of the four well-balanced capacitors reduces the AC leakage i_c considerably through DC control

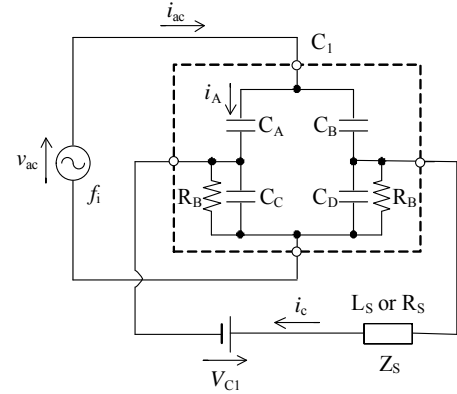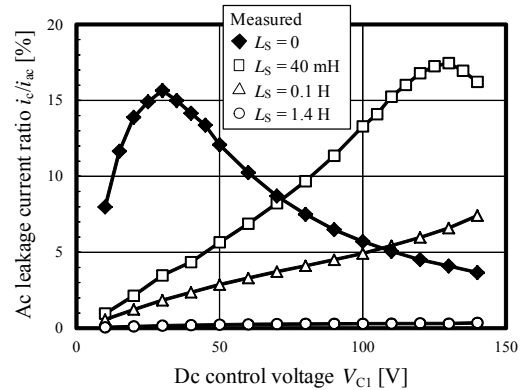Fig. 5. Measured data on the AC leakage ratio i_c/i_{ac} vs. the DC control voltage V_{C1} characteristics having the inductor L_S as series impedance device Z_S.

loop when V_{C1} is higher than the AC voltage v_{ac}. However, an impedance device Z_s needs to be inserted to suppress AC leakage, as shown in Fig. 4, when the AC voltage v_{ac} becomes high.

Figs. 5 and 6 show data on the AC leakage i_c from the VCD C_1 to the DC control voltage source V_{C1}. The current i_{ac} is the total AC current. These graphs depict the ratio i_c / i_{ac}. In this study, v_{ac} is sinusoidal. Its frequency f_i and amplitude equal 60 Hz and 10 V, respectively.

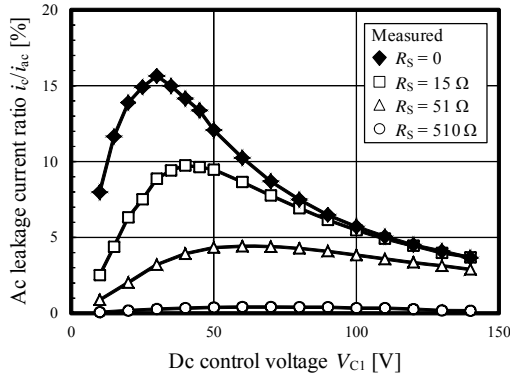As reference, the graph $L_S = 0$ in Fig. 5 or the graph $R_S = 0$ in Fig. 6 presents the data without Z_S. When V_{C1} is

Fig. 6. Measured data on the AC leakage ratio i_c/i_{ac} vs. the DC control voltage V_{C1} characteristics having the resistor R_S as series impedance device Z_S.
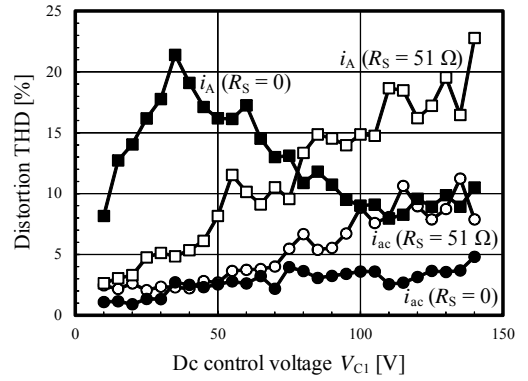

Fig. 7. Measured characteristics on the THD of the currents i_A and i_{ac} with the resistance R_S as parameter.
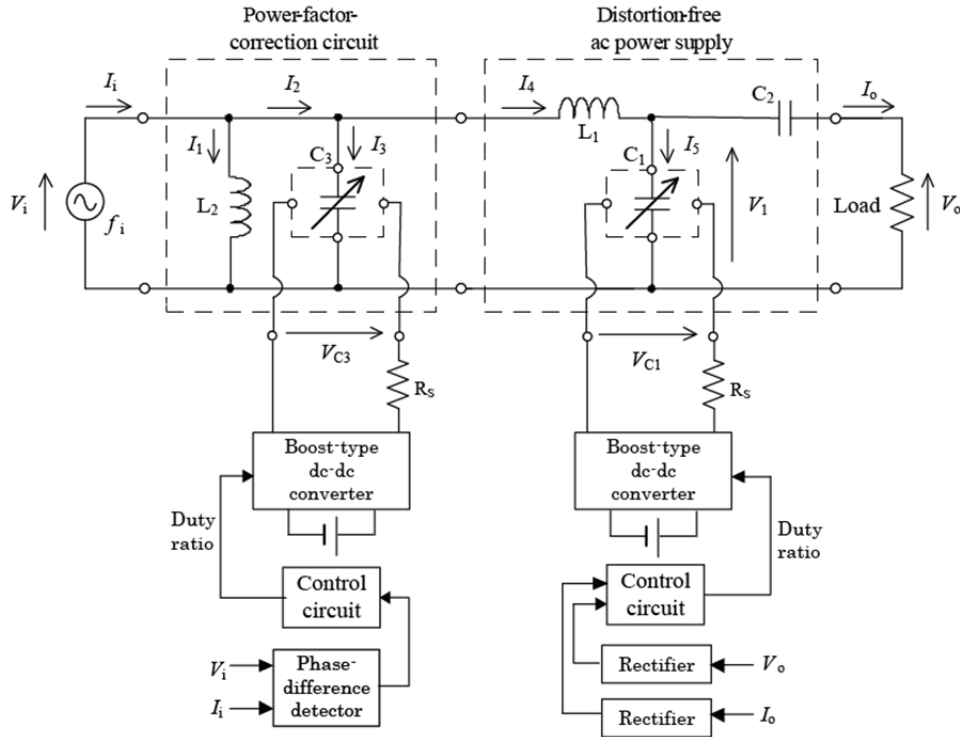

Fig. 8. PFC CV/CC AC power regulator by the use of VCDs.

approximately 30 V, the ratio i_c/i_{ac} has a maximum value. This condition corresponds to the maximum declivity in Fig. 2.

In Fig. 5, the inductor L_S is used as a series impedance device. Under a low V_{C1}, an inductor with relatively small inductance will be applicable.

The series component in Fig. 6 is the resistor R_S. Even if R_S is low, usage with a relatively high V_{C1} leads to good reduction characteristics on i_c/i_{ac}. A 51 Ω resistor is used below for the impedance device Z_S in consideration of cost, size, and weight.

IV. SUPPRESSION OF DISTORTION

For example, the capacitance C_A is a function of the voltage v_A. Given that v_A varies with the time t, C_A becomes a time-variant parameter. In this case, with respect to the capacitor C_A, the following relations are valid:

$$i_A = \frac{d}{dt}(C_A v_A) \tag{3}$$

$$i_A = C_A \frac{dv_A}{dt} + v_A \frac{dC_A}{dt} \tag{4}$$

The second term in the right part of Equ. (4) provides the information on distortion.

Fig. 7 shows the measured characteristics on total harmonic distortion (THD) with respect to the capacitor currents i_{ac} and i_A. From Fig. 4, i_A means the current that flows through the capacitor C_A. The amplitude of v_{ac} is set to 10 V. The THD of v_{ac} is approximately 0.17%, which is smaller than that of i_{ac} or i_A. In both cases of $R_S = 0$ and $R_S = 51 \Omega$, the distortion in i_{ac} becomes smaller than that in i_A. The
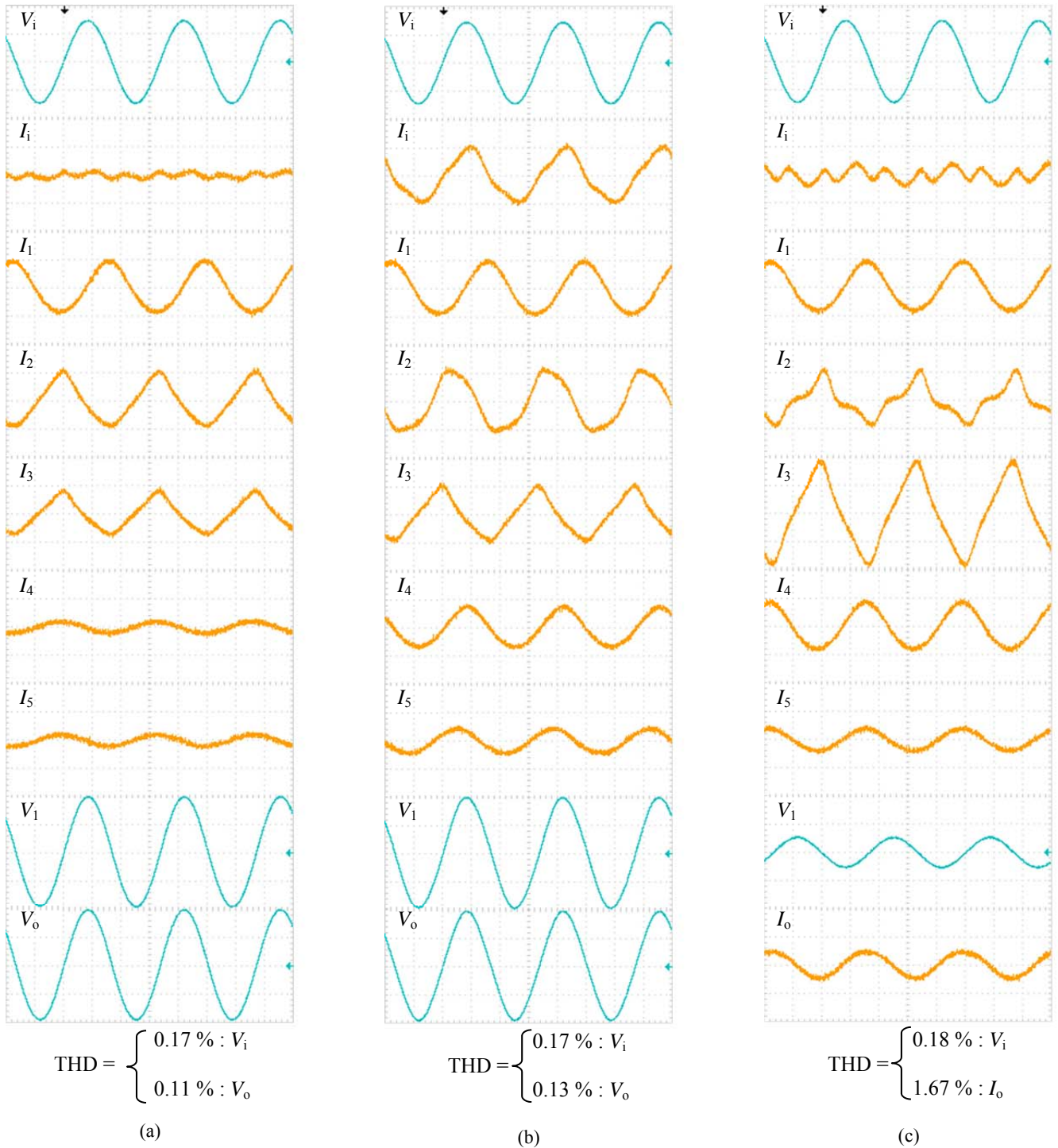
Fig. 9. Observed waveforms with the VCDs C_1, C_3, the sinusoidal input voltage V_i, and $R_S = 51\ \Omega$, where $V_i = 21$ V; vertical: 20 V/div for V_i, V_1, and V_o, 2 A/div for I_i, I_1–I_5, and I_o; horizontal: 5 ms/div: (a) $I_o = 0$ and $V_o = 28$ V (no load), (b) $I_o = 0.81$ A and $V_o = 28$ V (full load), and (c) $I_o = 0.81$ A and $V_o = 0$ (short-circuit load).

distortion in i_{ac} can be negligibly small particularly under the condition of $R_S = 0$. In this case, C_A and C_B and C_C and C_D are paralleled. The influence of nonlinearity can be compensated effectively. Even if $R_S = 51\ \Omega$, the total current i_{ac} becomes near sinusoidal.

V. EVALUATION OF THE DISTORTION IN AN AC POWER REGULATOR

Fig. 8 presents a CV/CC AC power regulator with input power factor correction (PFC) [8] as example of the
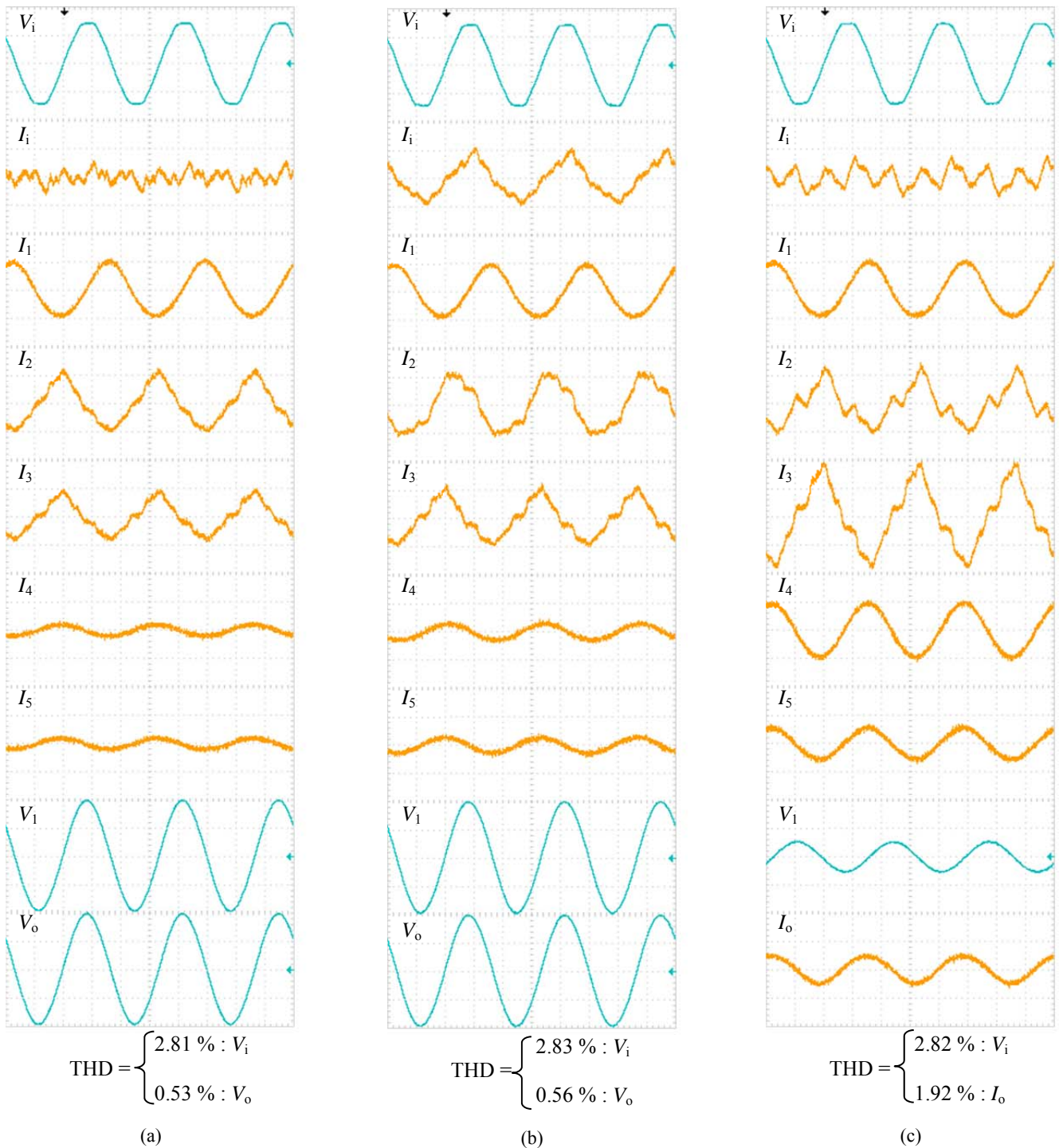
$$\text{THD} = \begin{cases} 2.81\,\% : V_i \\ 0.53\,\% : V_o \end{cases}$$

(a)

$$\text{THD} = \begin{cases} 2.83\,\% : V_i \\ 0.56\,\% : V_o \end{cases}$$

(b)

$$\text{THD} = \begin{cases} 2.82\,\% : V_i \\ 1.92\,\% : I_o \end{cases}$$

(c)

Fig. 10. Observed waveforms with the VCDs C_1, C_3, the commercial AC input voltage V_i, and $R_S = 51\ \Omega$. The others are the same as in Fig. 9.

application of VCDs. In this study, the capacitances C_1 and C_3 are variable. Load is assumed to be resistive.

The simplified block diagram for control circuit is also included in Fig. 8. Two boost-type DC–DC converters are utilized in this study for the high-speed drivers of two VCDs.

In the experimental circuit, the constant output voltage V_o = 28 V or the constant output current I_o = 0.81 A can be obtained against the input voltage V_i = 18–24 V. For the VCDs C_1 and C_3, the measured data on capacitance against DC control voltage are shown in Fig. 2.

$$\text{THD} = \begin{cases} 2.78\ \% : V_\text{i} \\ 0.32\ \% : V_\text{o} \end{cases}$$

(a)

$$\text{THD} = \begin{cases} 2.78\ \% : V_\text{i} \\ 0.27\ \% : V_\text{o} \end{cases}$$

(b)

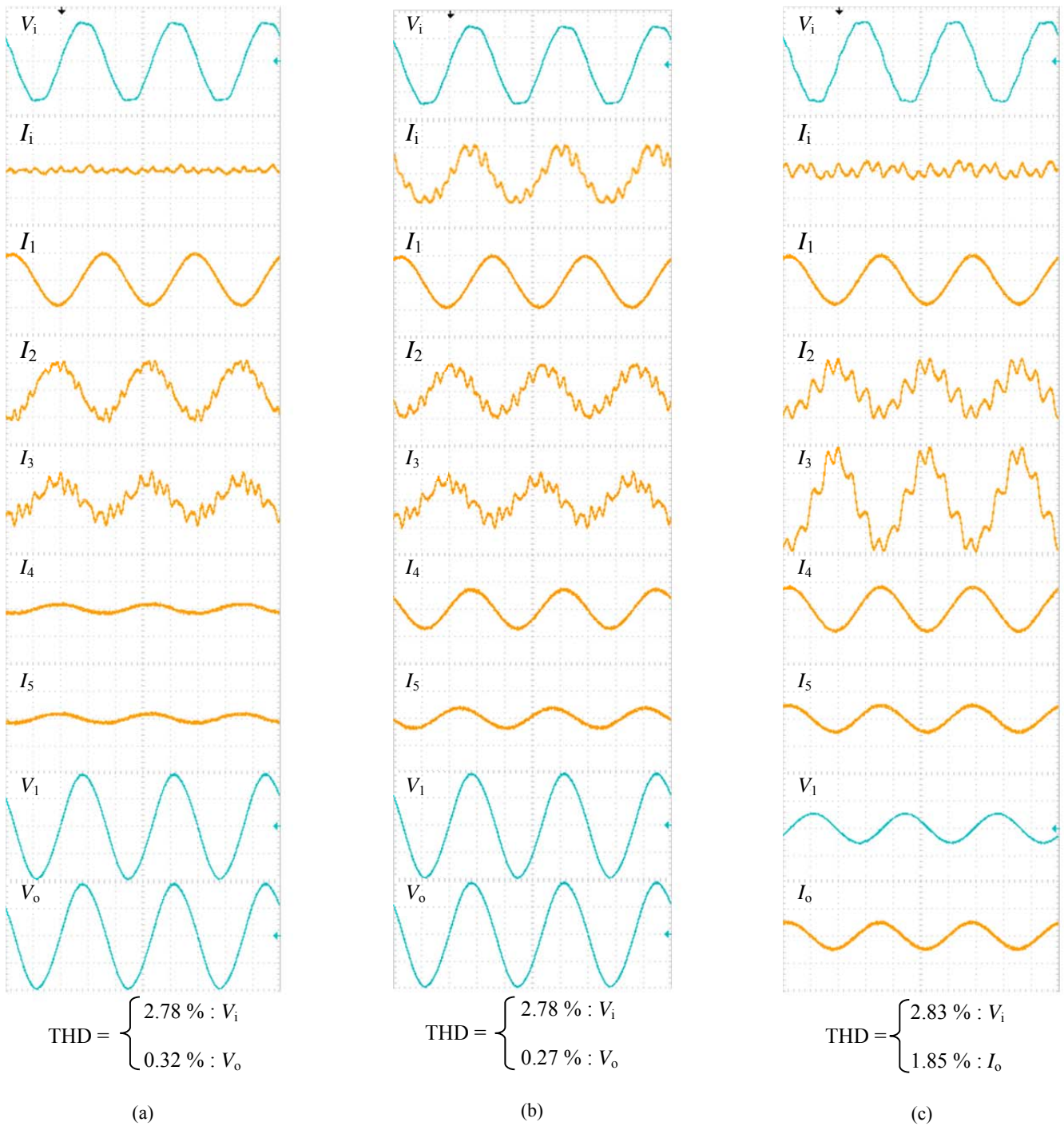$$\text{THD} = \begin{cases} 2.83\ \% : V_\text{i} \\ 1.85\ \% : I_\text{o} \end{cases}$$

(c)

Fig. 11. Observed waveforms with the film capacitors C_1, C_3 and the commercial AC input voltage V_i as reference. The others are the same as in Fig. 9.

The conditions are as follows: inductance of L_1, L_1 = 58 mH, loss resistance of L_1, $r_1 = 0.6\ \Omega$, inductance of L_2, L_2 = 35 mH, loss resistance of L_2, $r_2 = 0.2\ \Omega$, and capacitance of C_2, $C_2 = 290\ \mu\text{F}$.

Figs. 9–11 show the observed waveforms, where V_i, V_o, I_i, and I_o are the input voltage, the output voltage, the input current, and the output current, respectively. With respect to V_i, amplified sinusoidal voltage is used in Fig. 9. By contrast, V_i is furnished by a commercial AC in our laboratory for Figs. 10 and 11. In Figs. 9 and 10, R_S is equal to 51 Ω.

Fig. 9 presents the distortions generated when the input is a sinusoidal wave. A comparison between Figs. 9 and 10 implies that the THD of V_o or I_o does not gain much even if V_i is distorted. The high harmonic components in input voltage
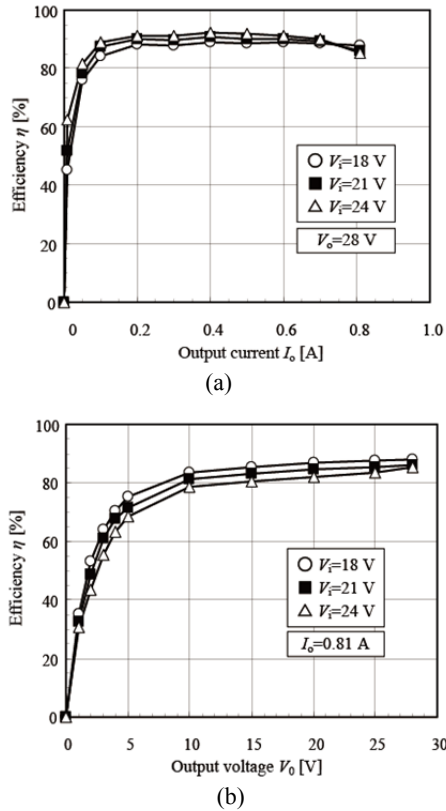
(a)

(b)

Fig. 12. Measured data of efficiency η with the VCDs C_1 and C_3: (a) CV region and (b) CC region.
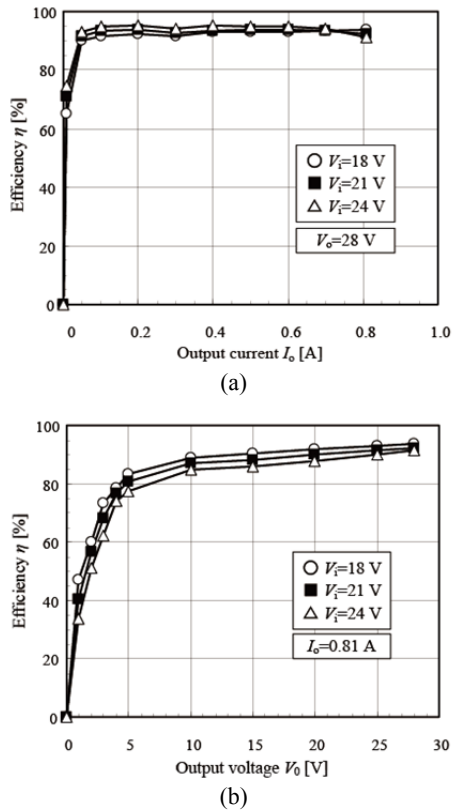

(a)

(b)

Fig. 13. Measured data of efficiency η with the film capacitors C_1 and C_3 as reference: (a) CV region and (b) CC region.

are effectively reduced.

As reference, Fig. 11 shows the observed waveforms using film capacitors of the same capacitance with VCDs. In this case, the included distortion is not derived from the VCDs. We suppose that the distortion is caused by magnetic devices and the high harmonic components of the commercial AC.

The measured values on THD are as follows:
(1) VCDs, sinusoidal AC input, and $R_S = 51\ \Omega$ (see Fig. 9).
    (a) No load; V_i: 0.17%, V_o: 0.11%.
    (b) Full load; V_i: 0.17%, V_o: 0.13%.
    (c) Short-circuit load; V_i: 0.18%, I_o: 1.67%.
(2) VCDs, sinusoidal AC input, and $R_S = 0$.
    (a) No load; V_i: 0.18%, V_o: 0.10%.
    (b) Full load; V_i: 0.19%, V_o: 0.11%.
    (c) Short-circuit load; V_i: 0.17%, I_o: 1.53%.
(3) Film capacitors and sinusoidal AC input.
    (a) No load; V_i: 0.18%, V_o: 0.09%.
    (b) Full load; V_i: 0.19%, V_o: 0.10%.
    (c) Short-circuit load; V_i: 0.17%, I_o: 1.45%.
(4) VCDs, commercial AC input, and $R_S = 51\ \Omega$ (see Fig. 10).
    (a) No load; V_i: 2.81%, V_o: 0.53%.
    (b) Full load; V_i: 2.83%, V_o: 0.56%.
    (c) Short-circuit load; V_i: 2.82%, I_o: 1.92%.
(5) VCDs, commercial AC input, and $R_S = 0$.
    (a) No load; V_i: 2.77%, V_o: 0.34%.
    (b) Full load; V_i: 2.76%, V_o: 0.33%.
    (c) Short-circuit load; V_i: 2.84%, I_o: 1.87%.
(6) Film capacitors and commercial AC input (see Fig. 11).
    (a) No load; V_i: 2.78%, V_o: 0.32%.
    (b) Full load; V_i: 2.78%, V_o: 0.27%.
    (c) Short-circuit load; V_i: 2.83%, I_o: 1.85%.

The data indicate that the distortion caused by VCDs is insignificant at $R_S = 51\ \Omega$ and $R_S = 0$.

Finally, the measured data on efficiency with VCDs and film capacitors are given in Figs. 12 and 13, respectively. In Fig. 13, VCDs are replaced with film capacitors of the same capacitance. The power loss in VCD is small.

VI. CONCLUSION

Inserting a suitable small-resistance resistor between the VCD and the DC control voltage source is effective for leakage current suppression. This resistor has almost no influence on capacitor current distortion.

Although the proposed VCD is made by using strong nonlinear characteristics, the waveform of the total current is not distorted considerably. The low distortion is due to the effective canceling of the high harmonic components by the internal currents in VCD.

In the proposed AC regulator for application in VCD, the distortion in input voltage is reduced by the effect of circuit configuration. Even if the AC input is a distorted voltage, such as the commercial AC voltage, the output waveform becomes close to a sinusoidal wave.

R<small>EFERENCES</small>

[1] R. J. Kakalec, "A feedback-controlled ferroresonant voltage regulator," *IEEE Trans. Magn.*, Vol. 6, No. 1, pp. 4-8, Mar. 1970.

[2] R. N. Basu, "A new approach in the analysis and design of a ferroresonant transformer," *IEEE Trans. Magn.*, Vol. 3, No. 1, pp. 43-49, Mar. 1967.

[3] A. Katsuki, K. Shirouzu, K. Harada, and M. Fujiwara, "Improved variable capacitance device and its applications to resonant converters," in *15th Int. Telecommunications Energy Conf.(INTELEC)*, Vol. 2, pp. 242-246, Sep. 1993.

[4] K. Harada, A. Katsuki, M. Fujiwara, H. Nakajima, and H. Matsushita, "Resonant converter controlled by Variable Capacitance Devices," *IEEE Trans. Power Electron.*, Vol. 8, No. 4, pp. 404-410, Oct. 1993.

[5] S. Igarashi, *Multi-layered Ceramic Capacitors*, Gakken-sha, 1988.

[6] M. W. Barsoum, *Fundamentals of Ceramics*, McGraw-Hill, 1997.

[7] S. O. Kasap, *Principles of Electrical Engineering Materials and Devices*, Rev., McGraw-Hill, 2000.

[8] A. Katsuki, K. Yoshimatsu, H. Tanoue, and Y. Sugimoto, "Distortion-free CV/CC AC power supply having the unity input power factor by the use of Variable Capacitance Devices," *International Journal of Renewable Energy Research*, Vol. 4, No. 3, pp. 641-646, Sep. 2014.

Akihiko Katsuki was born in Fukuoka, Japan in 1956. He received his B.Eng., M.Eng., and Ph.D. degrees from Kyushu University, Fukuoka, Japan in 1978, 1980, and 1983, respectively. In 1983, he was a research associate at Kyushu University. From 1988 to 1990, he was an associate professor at Kyushu University. In 1990, he was an associate professor at the Kyushu Institute of Technology, Fukuoka, Japan. Since 2013, he has been a professor at Nagasaki University, Nagasaki, Japan. His research interests include nonlinear power magnetics, power electronics, and communication circuits.

Takuya Oki was born in Hiroshima, Japan in 1988. He received his B.Eng. and M.Eng. degrees in Computer Science and Systems Engineering from Kyushu Institute of Technology, Iizuka, Fukuoka, Japan in 2010 and 2012, respectively. Since April 2012, he has been with Shindengen Electric Manufacturing Co., Japan. His current research interest is power electronics.